

# Dual-color visualization of *trans*-Golgi network to plasma membrane traffic along microtubules in living cells

Derek Toomre\*, Patrick Keller\*, Jamie White, Jean-Christophe Olivo and Kai Simons<sup>‡</sup>

Cell Biology/Biophysics Programme, European Molecular Biology Laboratory (EMBL), Meyerhofstrasse 1, 69117 Heidelberg, Germany

\*D.T. and P.K. contributed equally to this work

<sup>‡</sup>Author for correspondence (e-mail: simons@embl-heidelberg.de)

Dedicated to the memory of Dr Thomas Kreis

Accepted 29 October; published on WWW 8 December 1998

## SUMMARY

The mechanisms and carriers responsible for exocytic protein trafficking between the *trans*-Golgi network (TGN) and the plasma membrane remain unclear. To investigate the dynamics of TGN-to-plasma membrane traffic and role of the cytoskeleton in these processes we transfected cells with a GFP-fusion protein, vesicular stomatitis virus G protein tagged with GFP (VSVG3-GFP). After using temperature shifts to block VSVG3-GFP in the endoplasmic reticulum and subsequently accumulate it in the TGN, dynamics of TGN-to-plasma membrane transport were visualized in real time by confocal and video microscopy. Both small vesicles (<250 nm) and larger vesicular-tubular structures (>1.5 µm long) are used as transport containers (TCs). These TCs rapidly moved out

of the Golgi along curvilinear paths with average speeds of ~0.7 µm/second. Automatic computer tracking objectively determined the dynamics of different carriers. Fission and fusion of TCs were observed, suggesting that these late exocytic processes are highly interactive. To directly determine the role of microtubules in post-Golgi traffic, rhodamine-tubulin was microinjected and both labeled cargo and microtubules were simultaneously visualized in living cells. These studies demonstrated that exocytic cargo moves along microtubule tracks and reveals that carriers are capable of switching between tracks.

Key words: VSVG, GFP, Golgi, TGN, Cytoskeleton, Microtubule, Exocytosis

## INTRODUCTION

The *trans*-Golgi network (TGN) plays a critical role in sorting proteins to their final cellular destinations (reviewed by Traub and Kornfeld, 1997). Both polarized and non-polarized cells appear to share common molecular mechanisms and machinery in routing newly synthesized proteins to the plasma membrane (Yoshimori et al., 1996; Müsch et al., 1996), suggesting that several of the pathways may be common to many if not all cells (reviewed by Keller and Simons, 1997). While much progress on the characterization of the molecular machinery has been made (Traub and Kornfeld, 1997; Keller and Simons, 1997), identification of the carriers responsible in shuttling plasma membrane proteins from the TGN to the cell surface and their dynamics remains poorly understood. This information gap is largely due to inherent limitations of traditional approaches. For instance, many prior studies have involved biochemical assays, using either in vitro or permeabilized systems (e.g. Gravotta et al., 1990; Lafont et al., 1995; Yoshimori et al., 1996). Specifically, they monitor defined start and end points but are unable to identify intermediate steps or reveal complex transitory dynamics that occur in the single cell. An omnipresent concern of in vitro

studies is whether they adequately mimic conditions found in intact cells.

Other approaches to help identify carriers are immunofluorescence and electron microscopy (EM) (Griffiths et al., 1985; Ladinsky et al., 1994). Indeed, EM led to the initial identification of the TGN as an organelle (Griffiths and Simons, 1986). However, these static approaches are not able to determine the origin and fate of the transporting carriers. Moreover, as only a small percentage (~1-10%) (Nakata et al., 1998) of the cargo is transported at any given time, transitory cargo can be difficult to detect.

Alternative approaches include video time-lapse imaging of living cells by differential interference contrast (DIC) (Allen et al., 1981) or by epifluorescence, using exogenous fluorescently conjugated lipid probes such as NBD- or bodipy-ceramide (Pagano et al., 1991). However, these techniques have major caveats: DIC non-specifically monitors traffic of many organelles, while fluorescent lipid probes label several lipid species and undergo rapid photobleaching in living cells. Nevertheless, studies with these probes revealed that tubulovesicular elements may be involved in exocytic trafficking (Cooper et al., 1990).

A current technique exploits the intrinsic fluorescence of the

green fluorescent protein (GFP), as a tag for fusion proteins (for reviews see Lippincott-Schwartz and Smith, 1997; Tsien and Miyawaki, 1998). The GFP-tag is specific, sensitive, relatively photostable, and in many cases does not perturb normal trafficking or function of the protein. Recently, GFP-tagged temperature-sensitive mutants of VSVG were used to help dissect the dynamics of the early secretory pathway (Presley et al., 1997; Scales et al., 1997). Importantly, the transport of these VSVG-GFP chimeras can be synchronized since at the non-permissive temperature the VSVG reversibly misfolds and accumulates in the endoplasmic reticulum (ER) (Presley et al., 1997; Scales et al., 1997). Release from the temperature block caused the chimera to first concentrate in COPII-positive structures which exited the ER in pleiomorphic vesicular structures and were replaced by COPI-positive structures (Scales et al., 1997). Thus, GFP-chimeras have helped identify transitory carriers of novel morphology and provided valuable insight into the understanding of the early secretory pathway.

We have used a similar fusion protein (VSVG3-GFP) to monitor traffic between the TGN and plasma membrane in non-polarized cells. Our study shows that the major transport containers are not small vesicles (<250 nm) but rather much larger pleiomorphic structures including tubular structures. Moreover, late exocytic carriers appear to be capable of fission and fusion, suggesting that these structures are very dynamic and may be more complex than earlier models have assumed. Lastly, we address the role of the cytoskeletal elements in mediating late exocytic traffic and show direct evidence for the trafficking of exocytic cargo along microtubule highways.

## MATERIALS AND METHODS

### Cell culture

PtK<sub>2</sub> cells (ATCC CCL 56) were grown in MEM supplemented with 100 i.u./ml penicillin, 100 µg/ml streptomycin, 2 mM L-glutamine, 1× non-essential amino acids (Gibco BRL, Eggenstein, Germany), and 10% fetal calf serum (complete medium).

### VSVG3-GFP construction

VSVG3-GFP was constructed by fusing GFP to the C terminus of the full-length ts045-VSVG protein (GenBank accession number M11048). A DNA fragment encoding the VSVG protein without a stop codon was generated by PCR with an *EcoRI* site and consensus Kozak sequence at the 5'-end, and an in-frame *BamHI* site at the 3'-end. Primers used were 5'-TCG AAT TCG CCA TGA AGT GCC TTT-3' (forward primer, *EcoRI* site underlined) and 5'-GGT GGA TCC TTT CCA AGT CGG TT-3' (reverse primer, *BamHI* site underlined) to amplify the entire 1533 bp VSVG coding region, replacing the TAA stop codon with the GGA of the *BamHI* site. This PCR fragment was ligated into *EcoRI*-*BamHI* digested pEGFP-N1 (Clontech Laboratories, Palo Alto, CA). This construct inserts the amino acids DPPVAT between the last amino acid of VSVG and the start M of GFP. The 3 in VSVG3-GFP indicates that this was the third construct we tried; attempts to insert GFP between the cleaved signal sequence and the mature polypeptide of VSVG produced fusion proteins that were constitutively retained in the ER.

### Transient and stable transfection and preparation for microscopy

~70% confluent PtK<sub>2</sub> cells grown on 11 mm coverslips in a 35 mm dish were transiently transfected with VSVG3-GFP plasmid DNA

using calcium phosphate precipitation (Chen and Okayama, 1987) for 3 hours (3 µg DNA/ml per dish), washed twice with PBS, and incubated overnight (10-20 hours) at 39.5°C in complete medium lacking Phenol Red. To accumulate the chimera in the TGN, coverslips were placed in dishes containing a CO<sub>2</sub>-independent medium (Gibco BRL) supplemented with 20 µg/ml cycloheximide (Sigma) and incubated at 19.5°C for 2 hours. Subsequently, coverslips were transferred to an aluminum chamber containing fresh complete medium (without Phenol Red) and cycloheximide. For rhodamine-tubulin dual-color experiments 0.3 units/ml of Oxyrase™ (Oxyrase Inc., Ashland, OH) was added as an antioxidant. Coverslips were sealed with high vacuum silicon grease and immediately imaged on confocal or video microscopes as described below.

Stable VSVG3-GFP cell lines were obtained by calcium phosphate transfection and selection with 200 µg/ml G-418 (Gibco BRL). They were incubated overnight at 39.5°C with 5 mM sodium butyrate (Sigma) before each experiment. Behavior of transiently and stably expressing cells was generally similar (both in terms of Golgi/TGN accumulation and subsequent dynamic movement upon warmup to 32°C). However, transiently transfected cells were overall noticeably brighter, and were thus used in most studies (Figs 2-8).

### Microinjection

Rhodamine-tubulin was prepared using established methods (Hyman et al., 1991). Prior to microinjection, an aliquot of frozen rhodamine-tubulin (~30 mg/ml) was diluted 1:10 in ice-cold injection buffer (5 mM sodium phosphate, 100 mM KCl, pH 7.3) and centrifuged at 208,000 g for 8 minutes in a Beckman TLS-45 ultracentrifuge rotor to remove aggregates. The supernatant was microinjected into the cytosol of PtK<sub>2</sub> cells grown on coverslips in complete medium using an Eppendorf automated microinjection system (Rapp et al., 1996). For double microinjections, VSVG3-GFP plasmid DNA (20-50 µg/ml final) was added and both nuclei and cytoplasm were microinjected. After microinjection, cells were washed twice with PBS, replaced with complete medium lacking Phenol Red and allowed to recover overnight at 39.5°C. Subsequent accumulation in the TGN and processing was identical to that described above.

### Immunofluorescence

For colocalization studies of VSVG3-GFP and giantin, stably transfected cells grown on coverslips were blocked at temperatures indicated in Fig. 1. Subsequently, cells were washed with PBS (without Ca<sup>2+</sup> and Mg<sup>2+</sup>), fixed in 4% paraformaldehyde (PFA) at room temperature for 20 minutes, washed, blocked with 1% BSA in PBS, permeabilized for 5 minutes with 0.2% Triton X-100, washed with blocking buffer (1% BSA and 0.2% fish skin gelatin in PBS) and incubated with a 1:200 dilution of mouse anti-giantin antibodies (kind gift of H. P. Hauri, Biozentrum, Basel, Switzerland) for 30 minutes at 37°C. Coverslips were washed, incubated with a 1:100 dilution of rhodamine-labelled goat anti-mouse secondary antibodies for 30 minutes at 37°C, washed again, and mounted on slides with Moviol™ and viewed on a Leica inverted microscope. Immunofluorescence studies for actin and microtubules were performed similarly with the following differences: (i) cells were washed before fixation in PHEM buffer (60 mM Pipes, 25 mM Hepes, 10 mM EDTA, 2 mM MgCl<sub>2</sub>, pH 6.9), (ii) fixation was performed using either a brief 20 second pre-extraction in 0.1% Triton X-100 in PHEM buffer followed by fixation with 4% PFA in PHEM buffer or alternatively cells were fixed and permeabilized simultaneously using 0.1% Triton X-100, 0.05% glutaraldehyde, and 4% PFA in PBS. (Both procedures showed similar results although the actin cytoskeleton was slightly better preserved in the latter and was used for triple labeling studies.) (iii) Fixed coverslips were first stained with a 1:200 dilution of anti-α-tubulin (Amersham Life Science; Buckinghamshire, UK), and subsequently with a 1:100 dilution of both Cy5-labeled goat anti-mouse secondary antibody and Texas Red-phalloidin (Molecular Probes), and (iv) cells were imaged on a confocal microscope.

### Fluorescent microscopy, time-lapse imaging, and data processing

Confocal images (Figs 3, 7) of living cells were acquired on a Zeiss LSM 510 confocal microscope with a  $\times 63$  oil planapochromat lens (NA 1.4; Carl Zeiss, Inc) heated to 32°C. For single color GFP images the 488 nm line of an argon laser was used. Excitation and emission was monitored using a 505 nm long-pass filter. Samples were line scanned (typically 1.8  $\mu$ seconds/pixel,  $\sim 3$  seconds/frame) and power settings were minimized to avoid photobleaching. For triple color immunofluorescence experiments on fixed cells (GFP, rhodamine, and Cy5) excitation lines from 3 lasers were used (488 nm, 543 nm, 633 nm) and emission was monitored using the respective filters (505-530, 560-615, 650 long-pass).

Time-lapse epifluorescence video microscopy (Figs 1-2, 4-6) was performed using a Leica DM IRBE (Leica, Wetzlar, Germany) inverted microscope equipped with an automatic shutter, GFP and rhodamine filter blocks (Chroma Technology Corp., Brattleboro, VT), neutral density filters,  $\times 100$  oil-immersion objective (NA 1.3, Leica), sample heater (32°C) and a Hamamatsu C4742-95 (Hamamatsu Photonics, Japan) 12-bit high resolution CCD digital camera (0.134  $\mu$ m/pixel). Data were acquired on a Power Macintosh 8600/200 computer using OpenLab™ software (Improvision, Coventry, UK). Occasionally data was collected on a similar setup consisting of a Zeiss Axioskop microscope, a Cohu CCD camera, and NIH image acquisition software (NIH, Bethesda, MD).

Some images were processed to continuously subtract the previous frame, displaying only the difference between adjacent frames. Some images were RGB merged to create a composite temporal projection of several successive frames. Manual tracking and measurement of the fluorescence intensity of TCs was performed using OpenLab™ software. Automatic particle tracking was performed using a program developed in-house run on a Sun workstation which identifies, marks and tracks objects. It uses a Kalman filter and various parameters to determine if the objects follow tracks, and determines their instantaneous and average speed (Ngoc et al., 1997). Typically, in a single cell  $\sim 200$  vesicles/tubules were automatically identified. Tracked over 50 frames this corresponded to monitoring  $\sim 10,000$  events per cell.

## RESULTS

### Accumulation of VSVG3-GFP in the Golgi, and transport to the plasma membrane

The ts045 mutant of VSVG is reversibly misfolded and blocked in the ER at 39-40°C, but folds correctly and exits the ER at 31-32°C (Griffiths et al., 1985). Recently, several groups have attached a GFP-tag onto the C terminus of ts045-VSVG to create fusion proteins for monitoring secretory traffic (Presley et al., 1997; Scales et al., 1997). We have created a similar construct which differs slightly in the sequence connecting VSVG and GFP. When transiently or stably transfected PtK<sub>2</sub> cells were incubated at 39.5°C overnight the transfected cells displayed characteristic ER staining (not shown). To help further synchronize post-Golgi traffic, cells were incubated at 19.5°C for 2 hours. At this temperature exit from the TGN is blocked and secretory proteins accumulate in the TGN (Matlin and Simons, 1983; Griffiths et al., 1985). As expected VSVG3-GFP displayed characteristic perinuclear Golgi/TGN staining which by immunofluorescence colocalized with the Golgi marker giantin (Fig. 1A,B). Raising the temperature to 32°C for 1 hour caused VSVG3-GFP to exit the Golgi/TGN and reach the plasma membrane (Fig. 1C). After warmup for 1 hour (or longer) there was little

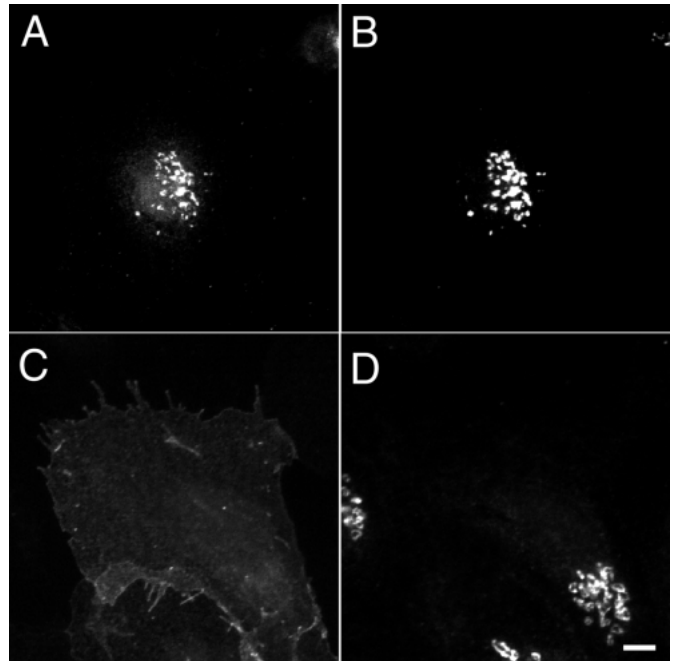


**Fig. 1.** Double labeling of VSVG3-GFP with Golgi markers using immunofluorescence microscopy. PtK<sub>2</sub> cells stably expressing VSVG3-GFP were incubated overnight at 39.5°C, blocked at 19.5°C for 2 hours and fixed immediately (A,B) or subsequently warmed up to 32°C for 1 hour and then fixed (C,D). Cells were permeabilized, labeled with anti-giantin antibodies, followed by rhodamine-conjugated secondary antibodies. GFP fluorescence is shown in A,C, while rhodamine labeling is shown in B,D. Bar, 5  $\mu$ m.

intracellular staining suggesting limited endocytosis of VSVG3-GFP.

### TGN-to-plasma membrane traffic in living cells: exocytic movement, docking and fusion

Having established that VSVG3-GFP accumulates in the Golgi at 19.5°C and reaches the surface upon warmup to 32°C, we choose to monitor exocytic traffic in living cells by time-lapse video microscopy. PtK<sub>2</sub> cells were used exclusively for these studies since they are both fairly large, typically 40-60  $\mu$ m, and extremely flat, typically less than 0.5  $\mu$ m thick in most of the periphery. Thus, in PtK<sub>2</sub> cells, post-Golgi exocytic movement takes place largely in a single focal plane. Typically several hundred frames were acquired with automatic shuttering to minimize exposure, at intervals ranging from 1 to 10 seconds. This allowed a total monitoring time ranging from a few minutes to  $\sim 30$  minutes. During imaging cells appeared healthy and displayed normal vitality signs such as filopodia extension/retraction and membrane ruffling. A typical time-lapse sequence is shown in Fig. 2A. Pleiomorphic vesicular structures were observed to move out of the Golgi region along curvilinear paths towards the cell periphery. Since these structures varied considerably in size and shape we will denote all such structures as transport containers or TCs. Generally, TCs moved towards the periphery along apparently random paths, often taking less than a few minutes.

After movement to the periphery, TCs sometimes were

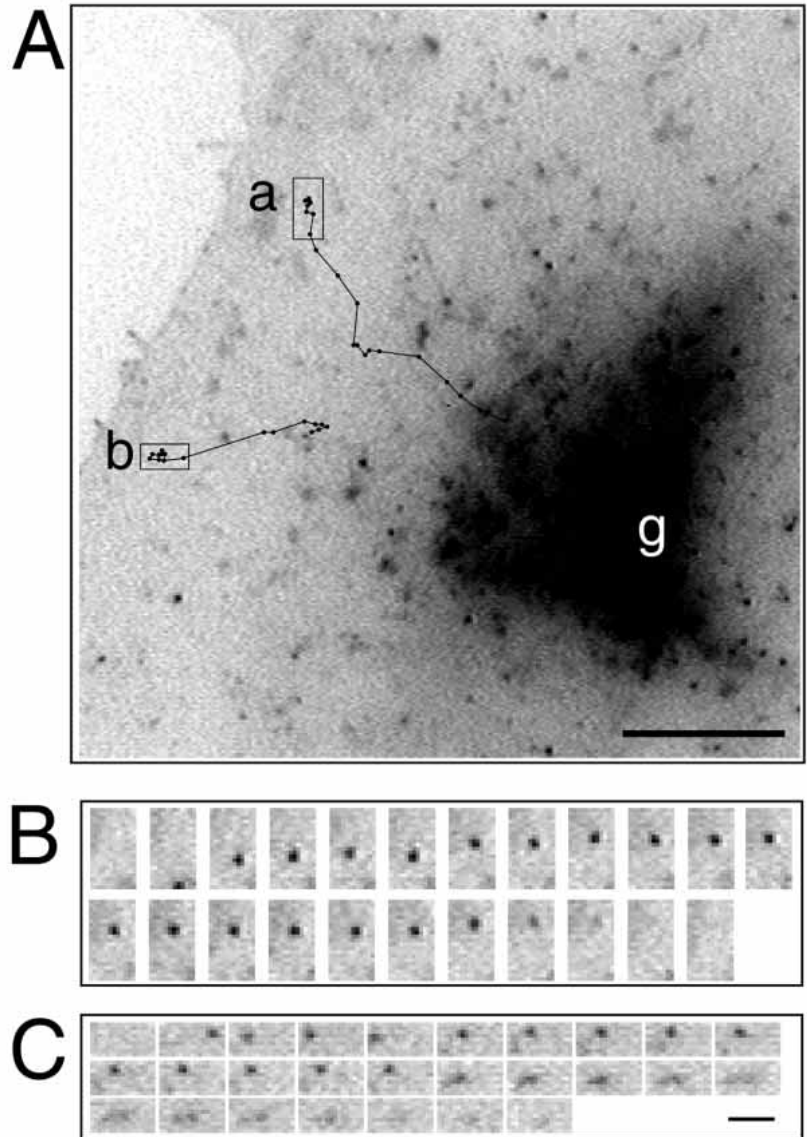


**Fig. 2.** Long time course shows movement of TCs to the cell periphery, tentative docking and fusion. VSVG3-GFP was accumulated in the TGN of transiently transfected PtK<sub>2</sub> cells for 2 hours at 19.5°C, warmed up to 32°C and imaged ~10 minutes post warm-up. Images (760 × 510 pixels) were collected every 4 seconds. The path of two typical TCs was traced as a line with dots indicating the position of the TC at 4 seconds intervals and overlaid on a single image; the general direction of movement was away from the Golgi (g) and towards the cell periphery (A). To highlight tentative docking and fusion events, B and C show enlargements of individual frames from regions a and b, respectively. Images were inverted for easier visualization. Bars: 5 μm (A); 1 μm (B,C).

stationary as if tethered/docked (Fig. 2B,C). Typically, the stationary phase lasted 45-60 seconds and then the signal would quickly disappear, suggesting that the TCs fused with the plasma membrane. The tentative fusion event was fast, below the time resolution of our instruments. It is unlikely that disappearance of TCs was caused by bleaching since weaker intensity TCs in the vicinity remained bright and many of these events were observed over long acquisition periods (20 minutes or more, imaged at 2-10 seconds intervals). We do not believe that these TCs had simply gone out of focus of the Z-plane since: (i) in the periphery where these events were observed these cells are extremely thin (<0.5 μm), (ii) using a wide field video microscope, objects that were obviously out of focus (e.g. the region above the nucleus) appeared fuzzy while when the TC fused it quickly vanished or 'puffed out', (iii) the fusion was in all cases observed to be preceded by a static phase (docking) making it unlikely to be a random movement in the Z-direction. Docking and fusion events have recently been observed in chromaffin cells (Steyer et al., 1997) and in neurons (Ryan et

al., 1997) using evanescent-wave fluorescence microscopy. These confirmed fusion events looked similar, namely the vesicle disappeared abruptly and often gave a diffuse cloud at the fusion site (Steyer et al., 1997). Since the tentative fusion we observed was rapid this suggests that most likely the entire TC fuses. Thus, our data suggest that indeed we are able to monitor TCs that exit the TGN, move outwards, dock and fuse.

### Post-Golgi exocytic traffic is highly dynamic and is capable of fission and fusion

What was also apparent from these video microscope studies was that some TCs were tubular, while others occasionally merged, suggesting possible fusion events (not shown). This was further investigated using laser confocal scanning microscopy since it was possible to make even thinner sections which increased the likelihood that movements were in a single plane. Large tubules occasionally emerged from the Golgi/TGN region (Fig. 3A). Sometimes these tubules or other large pleiomorphic structures divided into smaller structures

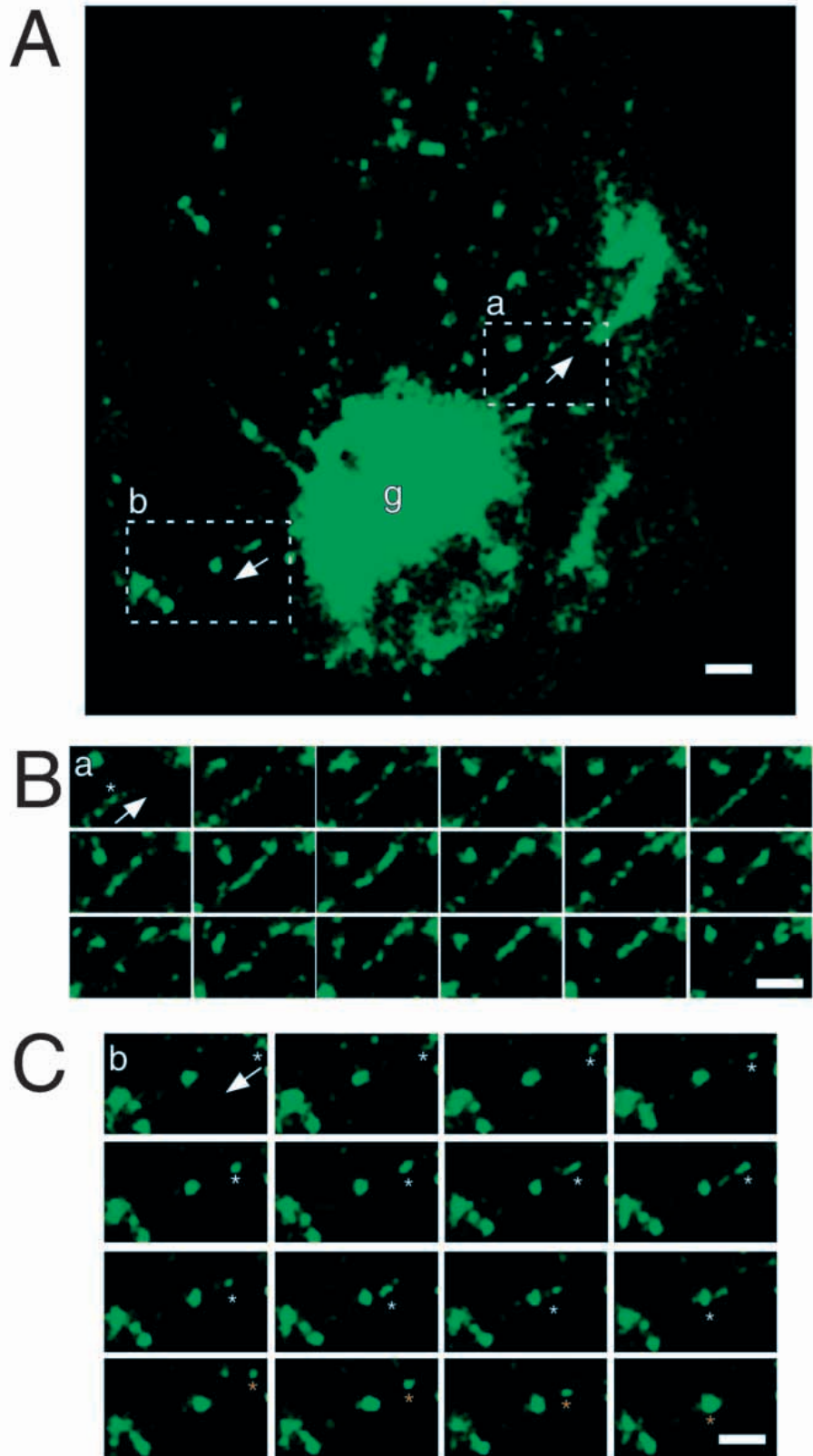


**Fig. 3.** Post-Golgi transport containers can exist in large highly-dynamic tubular structures. Time-lapse confocal images of VSVG3-GFP were acquired after shift to 32°C. A single image shows examples of large tubules or smaller vesicles emerging from the late Golgi/TGN (A). Enlargements of regions (a,b) are shown, respectively, in B and C. Time frames are 3.3 seconds apart. Arrows indicate the direction of movement. In B an asterisk marks the tip of a tubule which moves and divides into smaller vesicles in subsequent frames. In C the white asterisk follows the path of an individual vesicle which moves towards and appears to fuse with a static structure. An orange asterisk tracks the movement of another vesicle along a similar path. Bars, 5  $\mu$ m.

(Fig. 3B). Similarly, in living axons, transport tubules were observed to fragment as they moved along the axon (Nakata et al., 1998). The converse was also observed, namely the merging of TCs, presumably by fusion (Fig. 3C). Lastly, the

TCs varied widely in size ranging from <250 nm vesicles (maximum resolution of the light microscope) to tubules several  $\mu$ m in length (see Fig. 3B,C). Recent studies have documented that TCs of a large range of sizes exist in neurons

(Nakata et al., 1998); our findings corroborate these results in non-polarized cells.

**Both small vesicles and larger tubulovesicular structures transport newly synthesized proteins from the TGN to the plasma membrane**

Since our video microscope setup allowed much faster acquisition of high resolution images (up to 3 frames/second,  $0.134 \mu\text{m}/\text{pixel}$ ) than our confocal system, it was used to track short time-lapse post-Golgi movement of TCs (Fig. 4). A single

frame from the series is shown in Fig. 4A and a composite merge of 20 frames is shown in Fig. 4B; moving TCs appear as black streaks. In order to objectively identify and quantitate movement of TCs, an automatic particle tracking program was used to identify TCs in every frame. The projection of all particles (TCs) identified from 20 frames of a single cell is shown in Fig. 4C. Stringent threshold parameters were then applied which identified only those TCs moving along tracks (Fig. 4D). During this discrete time interval only a small amount of the TCs underwent long-range movements. It is also apparent

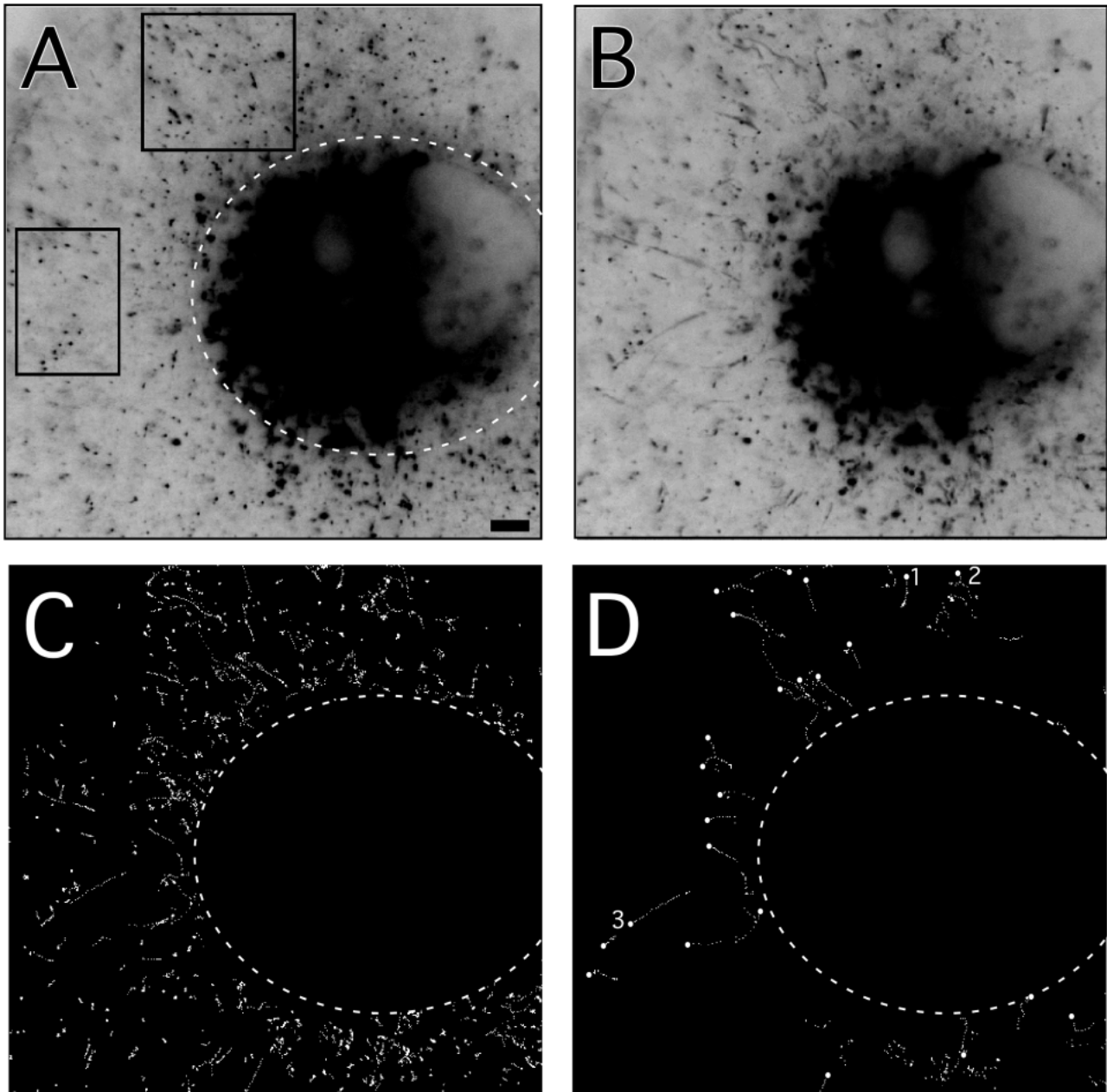


**Fig. 4.** Fast time-lapse video microscopy of post-Golgi exocytic trafficking shows movement along tracks. Images were acquired every 0.5 seconds. A single frame ( $0.134 \mu\text{m}/\text{pixels}$ ) is shown; boxes indicate regions enlarged in Fig. 6 (A). A composite projected merge of the first 20 frames; elongated 'smears' represent transport containers moving along curvilinear paths (B). Small white dots show all particles identified by automated particle detection (C). For clarity and to facilitate computation, a 'mask' (dotted circle) was applied to exclude movement in/around the Golgi. The program automatically identified TCs which moved along curvilinear tracks (D); the end point of each track is indicated with a larger dot. Note that most tracks are oriented towards the cell periphery. Tracks used for later graphs are labeled. Bar,  $5 \mu\text{m}$ .

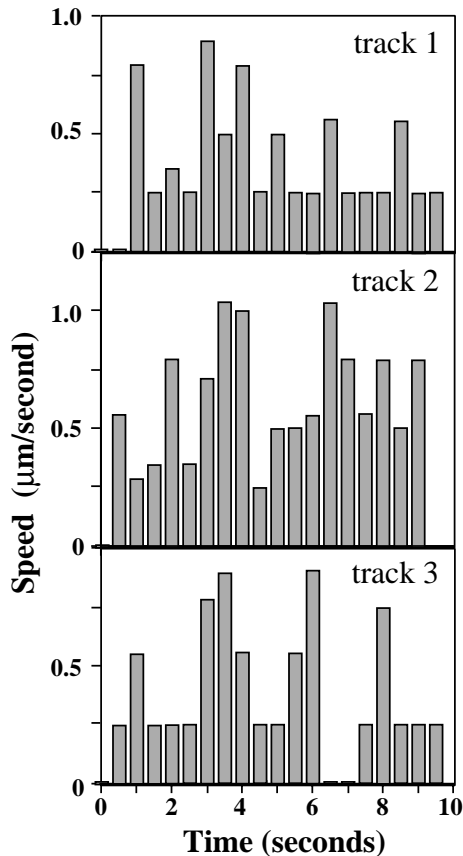


**Fig. 5.** Instantaneous speed of several TCs. The instantaneous speed of TCs moving on three representative tracks (marked in Fig. 4D) are shown.

that the majority of tracks are directed from the Golgi region out towards the periphery, as would be expected of late exocytic traffic. The advantage of the automatic tracking program is that it allows the majority of the moving TCs which move down tracks to be identified (given adequate signal/noise and spatial resolution). Manual tracking of all particles (assuming 200/cell) would require the plotting of ~6,000 events for a short 30 frame sequence. The average speed of TCs along tracks was  $\sim 0.66 \pm 0.18$   $\mu\text{m}/\text{second}$  and the maximum speed was  $\sim 1.17$   $\mu\text{m}/\text{second}$ . These values fit well with those observed for rapid motor driven exocytic movement (Lippincott-Schwartz, 1998). The values were similar for particles moving towards the Golgi and did not appear to differ with the size of the TCs (not shown). A graph of the instantaneous speed (between adjacent frames) along three of these tracks is shown in Fig. 5. The speeds were constant for periods up to  $\sim 1.5$  seconds, corresponding to  $\sim 1$   $\mu\text{m}$ , but occasionally underwent rapid changes, indicating that the cargo moves in a 'stop and go' fashion. Similar saltatory movements of secretory traffic have been observed in ER-to-Golgi transport and with other organelles such as peroxisomes (Wiemer et al., 1997).

What are the TCs responsible for moving the cargo out of the TGN to the plasma membrane? Specifically are they small vesicles, larger pleiomorphic tubular-like structures, or both? To help display the movement, regions from several frames of the same timelapse are shown (Fig. 6). Notably, both small

vesicles and larger tubular structures were observed to move. Although the majority of the TCs moved towards the periphery, a few moved towards the Golgi region (Fig. 6A, object #3). In some cases multiple TCs moved along a single track (Fig. 6B).

To help address which containers are responsible for transporting most of the cargo, all moving TCs in a given area ( $20 \times 20$   $\mu\text{m}$ ) were classified as either small vesicles (less than 250 nm, generally  $2 \times 2$  pixels) or tubule-like objects of larger dimensions. None of these objects had saturated pixels. The objects were manually selected, the fluorescent pixel intensity of each object was measured, and background fluorescence for equivalent areas was subtracted. This analysis showed that while the vesicles smaller than 250 nm were more numerous than the tubular elements ( $\sim 3$  to 1), the larger globular or tubular structures were much more fluorescent. Thus in moving TCs approximately one third of the total GFP-fluorescence was present in small vesicles while two thirds was present in the larger tubular/globular structures. This indicates that the large tubular elements are the major carriers in post-Golgi trafficking. We cannot, however, exclude the possibility that these larger tubular elements represent adjacent small vesicles that at the level of resolution of the light microscope appear as one object. However, we observed these large structures to move as a continuous unit for periods of several minutes suggesting that if this is the case these smaller subunits are tightly associated.

#### Localization of VSVG3-GFP along microtubules in fixed cells

The curvilinear paths along which TCs moved (see Figs 4, 6), suggested that cytoskeletal elements may serve as tracks for these movements. Thus, triple labeling was used to see if TCs were associated with microtubules (MT) or actin microfilaments. PtK<sub>2</sub> cells expressing VSVG3-GFP were incubated at 19.5°C, briefly warmed up to 32°C, fixed, permeabilized and processed for immunofluorescence. Triple color confocal imaging revealed that VSVG3-GFP was in close proximity to MT (see stereogram projection), but not associated with actin fibers (Fig. 7).

#### Movement of TCs along labeled microtubules in living cells

To address directly whether constitutive cargo moved along MT, we observed living cells double labeled with both VSVG3-GFP and rhodamine-labeled MT (Fig. 8). Basically, cells were monitored by video microscopy through a GFP filter for many frames, switched briefly to the rhodamine filter, then back to the GFP filter. By comparing MT images (before and after switching) we could ensure that minimal MT movement had occurred. After acquisition, images from a time-lapse sequence of VSVG3-GFP movement were merged into a single composite image (Fig. 8C). The curvy dotted line extending from the Golgi/TGN to the periphery represents a single TC which moved between successive frames (1 second). In order to display only the pixels which changed in intensity between frames (e.g. moving TCs), each individual frame had the previous frame subtracted. Thus, only material that moved between frames gave a signal. When all background subtracted frames were merged they produced the image in Fig. 8D. Relatively static structures, like the Golgi,

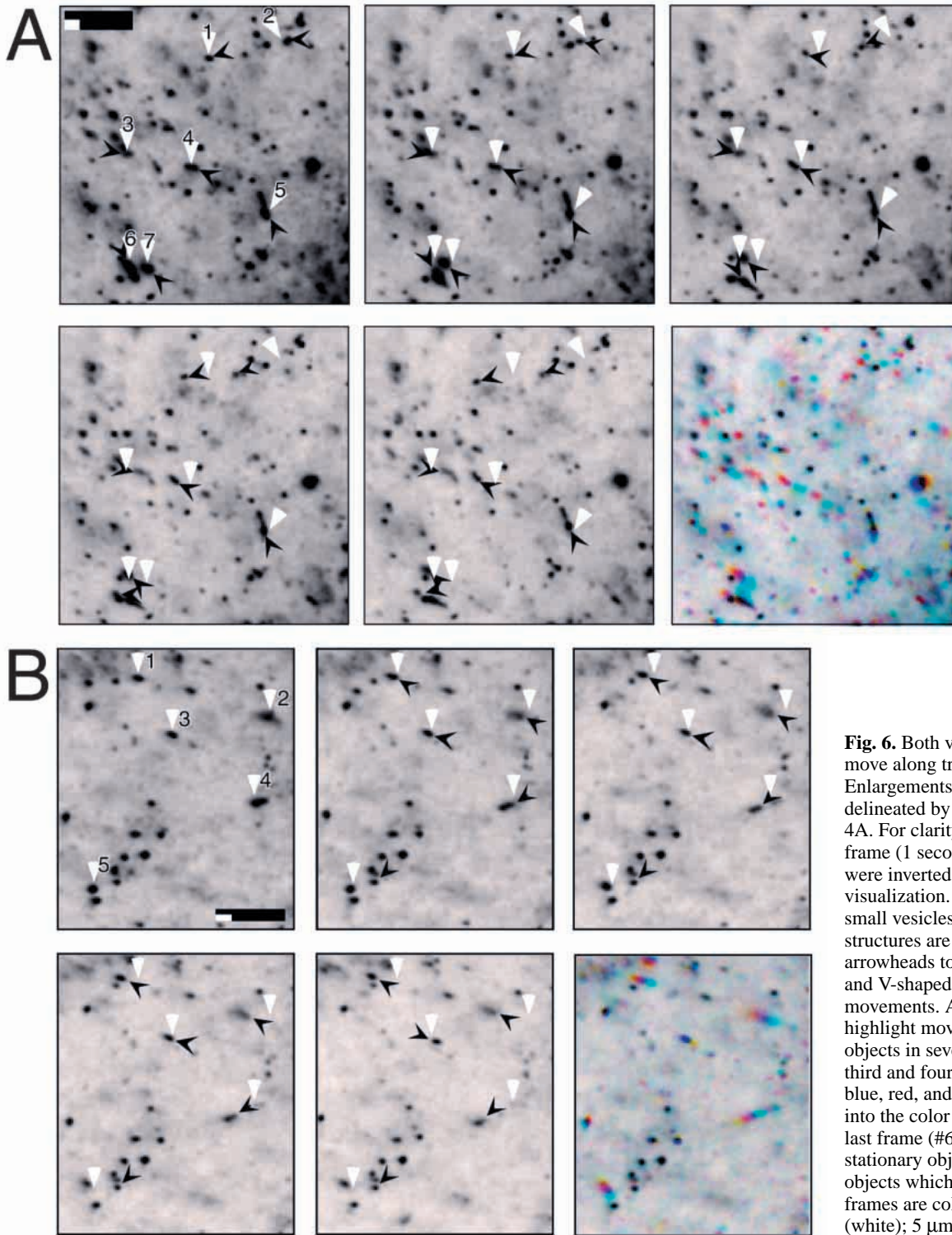


**Fig. 6.** Both vesicles and tubules move along tracks. (A and B) Enlargements of individual frames delineated by the two boxes in Fig. 4A. For clarity only every other frame (1 second) is shown. Images were inverted for easier visualization. Movement of several small vesicles and larger tubular structures are marked with arrowheads to indicate the start point and V-shaped arrows to track the movements. Alternatively, to highlight moving and stationary objects in several frames, the second, third and fourth frames were colored blue, red, and yellow and merged into the color projection shown in the last frame (#6A and B). Notably, stationary objects are black while objects which move during the 3 frames are colored. Bars: 1  $\mu\text{m}$  (white); 5  $\mu\text{m}$  (black).

are blank while very dynamic structures like the TCs are clearly seen extending along dotted curvy paths towards the periphery. When these are overlaid on the MT the S-curved paths of the majority of TCs coincided with the MT underneath (Fig. 8E-I). Thus, these results provide strong direct evidence that TCs which exit the TGN travel along MT towards the cell periphery. They complement indirect evidence for such an association obtained in other studies

(Cooper et al., 1990; Wacker et al., 1997). We observed directly TCs switching MT tracks (Fig. 8E-I) and often large relatively static tubules or globular structures (1  $\mu\text{m}$  or greater) were positioned near MT ends (compare Fig. 8E vs F); possibly due to an accumulation of cargo exiting the MT highways. In summary, these results provide direct evidence for the movement of TCs along MT in TGN-to-plasma membrane trafficking in unperturbed cells.

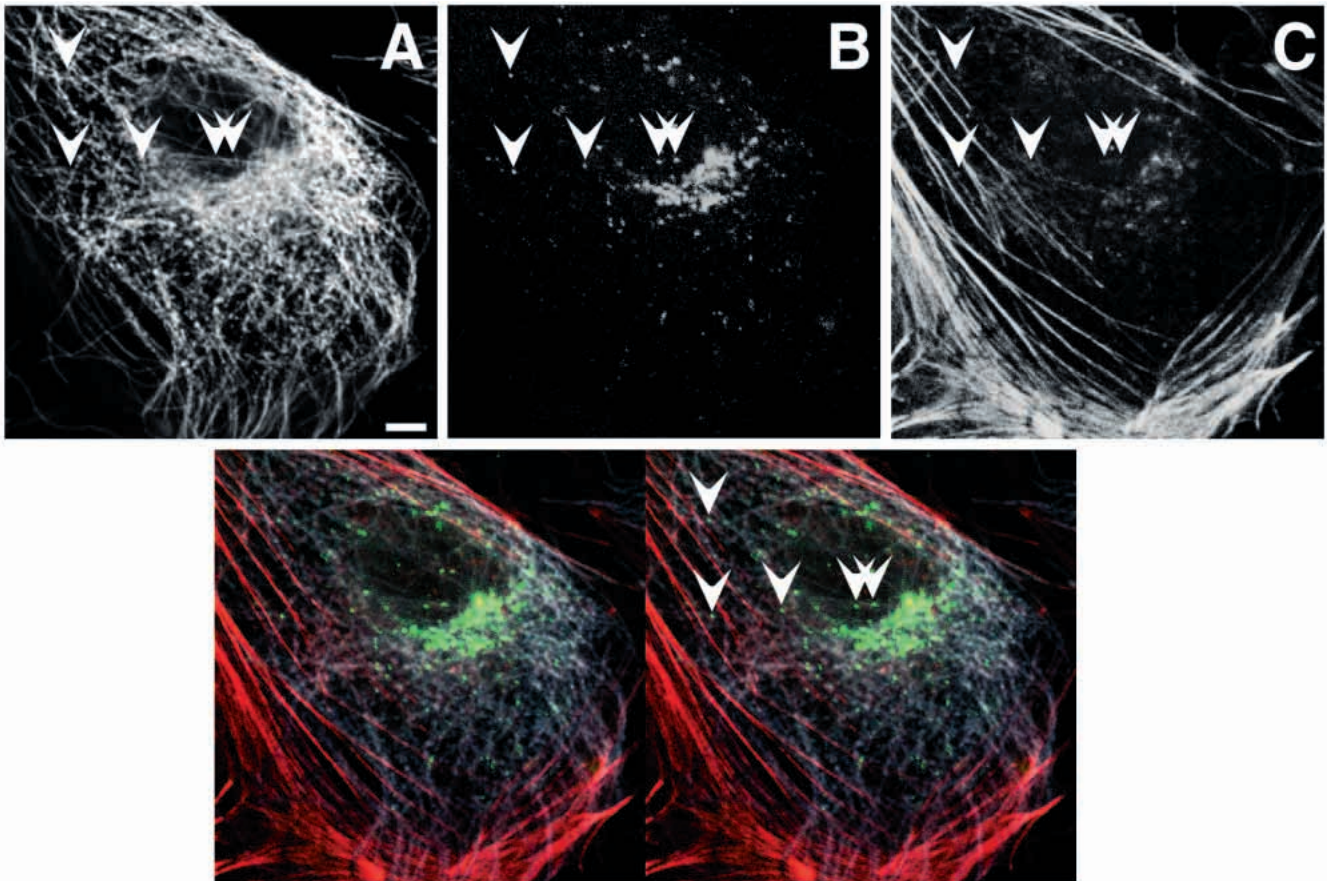


**Fig. 7.** Triple color stereogram shows the association of VSVG3-GFP transport complexes with microtubules but not actin cytoskeleton. VSVG3-GFP was accumulated in the TGN for 2 hours at 19.5°C, warmed to 32°C for 10 minutes, fixed, permeabilized, and processed for immunofluorescence using Texas Red-phalloidin and an anti-tubulin monoclonal antibody, followed by Cy5-labeled secondary antibody. Stacks of images were acquired as confocal Z-serial images (9 layers, 0.2  $\mu\text{m}$  thick, 512  $\times$  512 pixels) and projected using associated software. The individual Cy5 (MT), GFP, and Texas Red (actin) channels are shown, respectively, in A-C. Arrowheads indicate examples where VSVG3-GFP colocalizes with MT. The bottom 3-D stereogram merge of MT (white), VSVG3-GFP (green), and actin (red), shows even better the close juxtaposition of VSVG3-GFP with the underlying MT cytoskeleton. Bar, 5  $\mu\text{m}$ .

## DISCUSSION

We have explored the following related areas: (i) identification of the containers responsible for mediating post-Golgi traffic; (ii) visualization of the dynamics of late exocytic traffic in non-polarized cells; (iii) determination of the role of MT in directing traffic in unperturbed cells.

### Exocytic transport containers

What are the trafficking containers? Unlike biochemical studies which categorize 'vesicles' by their associated molecular machinery and physical properties, we have approached this question by monitoring the dynamic morphology of living cells. Data from our study suggest that both small vesicles (less than 250 nm in diameter, the level of resolution at the light microscope) as well as considerably larger tubular/globular structures (often larger than 1  $\mu\text{m}$ ) are involved in transporting late secretory cargo in non-polarized cells.

Using VSVG-GFP as a probe, large fluorescent tubules were also observed in post-Golgi exocytic traffic in COS cells (J. Lippincott-Schwartz, personal communication). The

identification of larger structures challenges the classical view that only small vesicles are involved in mediating late exocytic traffic; only recently with the advent of GFP technology have larger TCs been identified and shown to play an important role in the early secretory pathway (Presley et al., 1997; Scales et al., 1997). Moreover, we quantitated the amount of fluorescent cargo in these larger moving structures and showed that indeed they transported the majority of cargo. But how does one reconcile the observation that *in vitro* small vesicles are predominately observed? One possibility is that biochemical fractionation techniques may have simply enriched small vesicles. A second possibility is that since *in vivo* these structures are capable of fission (Fig. 3), fragmentation may occur during isolation. On the other hand, diverse sizes of TCs have been observed by EM (Griffiths et al., 1985; Ladinsky et al., 1994) and more recently by confocal laser scanning microscopy of axons (Nakata et al., 1998). Curiously, in contrast with our results and those of GFP-tagged membrane proteins in axons, studies with GFP-tagged chromogranin showed only vesicles and no tubules (Wacker et al., 1997). These differences suggest various possibilities: secretory and membrane-bound proteins may sort into different TCs or

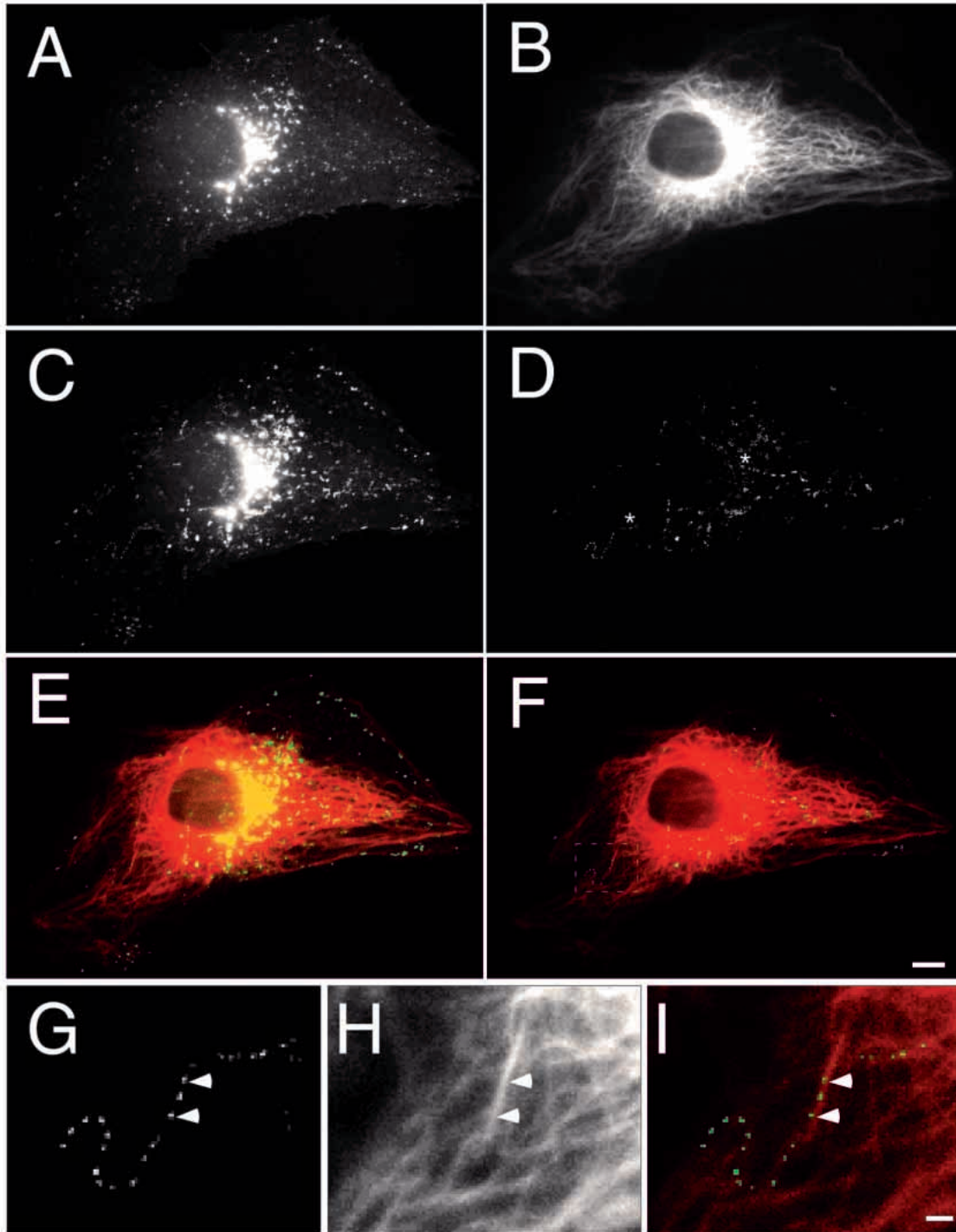


**Fig. 8.** Live dual-color imaging of VSVG3-GFP and rhodamine-tubulin shows direct movement of VSVG3-GFP along microtubules. PtK<sub>2</sub> cells on coverslips were microinjected with both VSVG3-GFP and rhodamine-tubulin into the nucleus and cytosol, respectively. Cells were held overnight at 39.5°C, then 2 hours at 19.5°C, then warmed to 32°C and monitored by a conventional fluorescence microscope equipped with rhodamine and GFP filters (sequence acquired ~10 minutes post-warmup). Images were acquired every second (~100 millisecond exposure) in the GFP channel using shutters to minimize bleaching. Approximately every 15 frames the rhodamine channel was monitored for 1 or 2 frames. A single image of VSVG3-GFP from the beginning of the sequence is shown in A. A merged image of only the microtubules at the start and end of the sequence is shown in B. A series of 25 frames of VSVG3-GFP were merged to give the composite projection shown in C. Two frame running subtraction of successive images shows only the moving VSVG3-GFP (D). Two snake-like tracks of VSVG3-GFP are apparent; the start point is indicated with white asterisks. (E) A merge of B and C, (F) a merge of B and D. An enlargement of the boxed region in F is shown in I. The GFP and rhodamine channels are shown in G and H. (H) MT are shown in white for better contrast. Examples of temporal and spatial co-localization are marked with arrowheads. Bars: 5  $\mu$ m (F); 1  $\mu$ m (I).

different cell types may vary in their propensity for tubule formation.

Moreover, is it possible that these globular or tubular structures are actually endosomes (Futter et al., 1995; Leitingner et al., 1995)? Other studies have indicated that the exocytic TCs were not endosomes (Wacker et al., 1997; Nakata et al., 1998). We tested for overlap with the endosomal system by dual color visualization of VSVG3-GFP and fluorescently tagged fluid phase markers or lectins. Our data indicated little overlap of exocytic and endocytic cargo; however, we cannot exclude the possibility that brief passage through a portion of the endocytic pathway may have occurred (D. Toomre and K. Simons, unpublished data).

Having established that large tubulovesicular carriers play a major role in post-Golgi exocytic trafficking, what can this tell us about their function? Interestingly, *in vitro* studies showed that when Golgi membranes were added to immobilized MT and monitored by DIC video microscopy, tubulovesicular structures formed and moved along MT tracks (Allan and Vale, 1994). These structures consisted of tubules with a discrete globular 'head' domain (also observed by EM). The authors noted that often the globular head was enriched for very low density lipoprotein particles and secretory cargo and would appear to pull traffic down the MT and occasionally it would fragment from the tubule and continue moving. Many of our videos showed similar structures (for example see Fig. 6A, objects #5, 6). We observed tubules moving, flipping direction, and occasional separation of the 'head' domains (data not shown), suggesting that motors and cytoskeletal elements may be involved in their formation. Interestingly, recent *in vitro* studies showed that dynamin is sufficient for converting liposomes into long membrane tubules which vesiculate upon addition of GTP (reviewed by McNiven, 1998). Obviously, these and our results challenge the simple view of vesiculation driven by coat envelopment being the major mechanism for TC morphogenesis.

### Dynamics of TGN-to-plasma membrane transport

In our study post-Golgi exocytic TCs had an average speed of  $\sim 0.7 \mu\text{m}/\text{second}$  and a maximal speed of  $1.2 \mu\text{m}/\text{second}$ . This is consistent with values obtained from other studies which ranged from  $0.3\text{--}1 \mu\text{m}/\text{second}$  (Cooper et al., 1990; Nakata et al., 1998; Wacker et al., 1997). Variations of 'instantaneous' speed (between two frames) indicated that the TCs move in a saltatory fashion, alternating between periods of fast movement and pauses (Fig. 5). The TCs moved along curvilinear paths, generally towards the periphery (see Figs 2, 4). Automatic computer tracking enabled us to readily determine and plot all particle movements associated with tracks without bias (see Fig. 4D). The automatic particle tracking and analysis of several thousand points employed in this study may explain why we were able to observe general outward movements of tubules and vesicles that may have been difficult to spot with manual tracking. On the other hand, in the study of ER-to-Golgi dynamics of VSVG-GFP (Presley et al., 1997) TC paths were clearly inward. In our study, general movements out of the Golgi region along curvilinear tracks (proven herein to be MT) suggest that the plus end directed MT motor kinesin may dominate. Perhaps saltations, hovering and bidirectional movement may be due to dynein and kinesin motors on the same TC; however, additional studies would be required to test

this possibility directly. Lastly, during exocytic trafficking, we occasionally observed TCs undergoing putative fission (similar to post-Golgi trafficking in neurons; Nakata et al., 1998), and even fusion, suggesting that these processes are highly dynamic.

### Post-Golgi secretory traffic occurs along microtubules

To date, most evidence for the involvement of MT in mediating TGN-to-plasma membrane traffic is indirect (Lippincott-Schwartz, 1998). Most studies have used drugs to depolymerize MT (Wacker et al., 1997; Bloom and Goldstein, 1998; Lippincott-Schwartz, 1998). However, it is worth reiterating some major caveats of drug depolymerization studies: (i) if an effect is seen (transport is blocked), one must determine if it is due to a primary effect or a secondary effect (such as disrupting normal cellular architecture), and (ii) if no effect or a slight effect is seen one must determine if an alternate non-physiological pathway is used instead (Sheetz, 1996; Bloom and Goldstein, 1998). Notably, nocodazole treatment has had mixed results on TGN-to-plasma membrane traffic, sometimes preventing surface delivery, other times showing no effect or a decrease in the kinetics (Cole and Lippincott-Schwartz, 1995; Bloom and Goldstein, 1998). The use of non-physiological pathways after drug treatment may be particularly relevant in flat tissue culture cells where the closest distance from the TGN to the overlying plasma membrane may only be a couple of  $\mu\text{m}$ . Once MT are removed, vesicles could potentially reach the plasma membrane by random upward diffusion, estimated to take under 15 minutes. In fact, we observed that after treatment with nocodazole for one hour on ice, upon warmup VSVG3-GFP was still able to reach the cell membrane. Confocal Z-sections showed a diffuse cloud of vesicles around the nucleus, not seen in mock treated cells (data not shown). These observations coupled with the fact that MT in PtK<sub>2</sub> cells are stable and difficult to depolymerize (Bre et al., 1987) enamored us to try a more direct approach.

We labeled all MT with rhodamine tubulin and imaged simultaneously or with minimal temporal separation both VSVG3-GFP and the labeled MT. Importantly, these studies clearly showed movement of VSVG3-GFP down curved MT tracks (Fig. 8). Generally, no specific MT were obviously preferred as tracks. In fact carriers were observed to switch MT during movement. Occasionally some MT situated close to the Golgi/TGN showed heavy traffic, however, whether this is due to the spatial positioning or a modification of these MT (e.g. stabilization) is not clear. There is evidence for the involvement of stable MT in ER-to-Golgi traffic (Mizuno and Singer, 1994) and also in Golgi-to-cell surface traffic in WIF-B cells (Pous et al., 1998). The role of stable MT in late exocytic traffic is likely not easily addressed in PtK<sub>2</sub> cells since many stable MT are present, hence it remains an open question. Thus, as a working model we favor that late exocytic traffic down MT is mainly a stochastic process, but plus end directed movement (presumably kinesin driven) predominates. This causes a general movement of traffic towards the periphery where it subsequently docks and fuses with the plasma membrane.

One major unresolved issue is the role of the actin cytoskeleton in this process. Notably, cortical actin is

believed to act as a physical barrier which must be breached in order for fusion to occur. We saw no association of VSVG3-GFP with stress fibers, although arguably due to the prevalence of F-actin and the resolution of light microscopy, transient associations with cortical actin would be difficult to spot. Cytochalasin D had no effect on surface delivery of VSVG3-GFP (actin shown to be depolymerized; data not shown). However, as mentioned above, a caveat of these drugs is that once the cortical actin barrier is removed, carriers might jump (non-physiologically) across the gap by diffusion. Finally, anti-P200/myosin II antibodies were reported to have no effect on TGN-to-plasma membrane trafficking in vivo (Ikonen et al., 1996; Pepperkok et al., 1998). Thus, if actin cytoskeleton is involved in exocytosis its role in vivo remains obscure.

### Perspectives

These studies suggest that TGN-to-plasma membrane traffic is much more complex and dynamic than most 'vesicle' models (Traub and Kornfeld, 1997) have predicted. Our studies suggest that large tubulovesicular structures play an important role in late trafficking events. The molecular mechanisms of how these structures form in vivo is still unknown, but diverse evidence from EM (McNiven, 1998), biochemical studies (Keller and Simons, 1997) and recently video imaging (Lippincott-Schwartz and Smith, 1997) are beginning to synergistically merge. Perhaps soon they may help explain how these remarkable tubules and head domains form, segregate and move in the cell. Our data directly prove that TCs ride down MT highways in the last steps of the exocytic pathway. Moreover, these technological advances have allowed us to glimpse at fleeting dynamic processes such as budding, docking and fusion. The next challenge will be to simultaneously monitor different dynamic processes, such as apical and basolateral sorting in living cells. Dual labeling with multi-colored GFPs (Lippincott-Schwartz and Smith, 1997; Tsien and Miyawaki, 1998) should facilitate exploration of these exciting new vistas.

We particularly acknowledge Improvion and Leica for generously providing equipment and support, Regis Tournebize for providing rhodamine-tubulin, Ann Atzberger for cell sorting, Frederic Briquet-Laugier for development of the automated tracking program and Mari Kawaguchi for secretarial assistance. D.T. was supported by a Marie Curie Research grant (no. ERBFMBICT961424), P.K. by a Training and Mobility of Researchers grant of the European Community (83EU-044159) and K.S. by a grant from the Deutsche Forschungsgemeinschaft (SFB 352).

### REFERENCES

- Allan, V. and Vale, R. (1994). Movement of membrane tubules along microtubules in vitro: evidence for specialised sites of motor attachment. *J. Cell Sci.* **107**, 1885-1897.
- Allen, R. D., Allen, N. S. and Travis, J. L. (1981). Video-enhanced contrast, differential interference contrast (AVEC-DIC) microscopy: a new method capable of analyzing microtubule-related motility in the reticulopodial network of *Allogromia laticollaris*. *Cell Motil.* **1**, 291-302.
- Bloom, G. S. and Goldstein, L. S. (1998). Cruising along microtubule highways: how membranes move through the secretory pathway. *J. Cell Biol.* **140**, 1277-1280.
- Bre, M., Kreis, T. and Karsenti, E. (1987). Control of microtubule nucleation and stability in Madin-Darby canine kidney cells: the occurrence of noncentrosomal, stable detyrosinated microtubules. *J. Cell Biol.* **105**, 1283-1296.
- Chen, C. and Okayama, H. (1987). High-efficiency transformation of mammalian cells by plasmid DNA. *Mol. Cell Biol.* **7**, 2745-2752.
- Cole, N. B. and Lippincott-Schwartz, J. (1995). Organization of organelles and membrane traffic by microtubules. *Curr. Opin. Cell Biol.* **7**, 55-64.
- Cooper, M. S., Cornell-Bell, A. H., Chernjavsky, A., Dani, J. W. and Smith, S. J. (1990). Tubulovesicular processes emerge from trans-Golgi cisternae, extend along microtubules, and interlink adjacent trans-Golgi elements into a reticulum. *Cell* **61**, 135-145.
- Futter, C. E., Connolly, C. N., Cutler, D. F. and Hopkins, C. R. (1995). Newly synthesized transferrin receptors can be detected in the endosome before they appear on the cell surface. *J. Biol. Chem.* **270**, 10999-11003.
- Gravotta, D., Adenisk, M. and Sabatini, D. (1990). Transport of influenza HA from the trans-Golgi network to the apical surface of MDCK cells permeabilized in their basolateral plasma membranes: energy dependence and involvement of GTP-binding proteins. *J. Cell Biol.* **111**, 2893-2908.
- Griffiths, G., Pfeiffer, S., Simons, K. and Matlin, K. (1985). Exit of newly synthesized membrane proteins from the trans cisterna of the Golgi complex to the plasma membrane. *J. Cell Biol.* **101**, 949-964.
- Griffiths, G. and Simons, K. (1986). The trans Golgi network: sorting at the exit site of the Golgi complex. *Science* **234**, 438-443.
- Hyman, A., Drechsel, D., Kellogg, D., Salsler, S., Sawin, K., Steffen, P., Wordeman, L. and Mitchison, T. (1991). Preparation of modified tubulins. *Meth. Enzymol.* **196**, 478-485.
- Ikonen, E., Parton, R. G., Lafont, F. and Simons, K. (1996). Analysis of the role of p200-containing vesicles in post-Golgi traffic. *Mol. Biol. Cell* **7**, 961-974.
- Keller, P. and Simons, K. (1997). Post-Golgi biosynthetic trafficking. *J. Cell Sci.* **110**, 3001-3009.
- Ladinsky, M. S., Kremer, J. R., Furcinitti, P. S., McIntosh, J. R. and Howell, K. E. (1994). HVEM tomography of the trans-Golgi network: structural insights and identification of a lace-like vesicle coat. *J. Cell Biol.* **127**, 29-38.
- Lafont, F., Simons, K. and Ikonen, E. (1995). Dissecting the molecular mechanisms of polarized membrane traffic: reconstitution of three transport steps in epithelial cells using streptolysin-O permeabilization. *Cold Spring Harbor Symp. Quant. Biol.* **LX**, 753-762.
- Leitinger, B., Hille-Rehfeld, A. and Spiess, M. (1995). Biosynthetic transport of the asialoglycoprotein receptor H1 to the cell surface occurs via endosomes. *Proc. Nat. Acad. Sci. USA* **92**, 10109-10113.
- Lippincott-Schwartz, J. and Smith, C. L. (1997). Insights into secretory and endocytic membrane traffic using green fluorescent protein chimeras. *Curr. Opin. Neurobiol.* **7**, 631-639.
- Lippincott-Schwartz, J. (1998). Cytoskeletal proteins and Golgi dynamics. *Curr. Opin. Cell Biol.* **10**, 52-59.
- Matlin, K. S. and Simons, K. (1983). Reduced temperature prevents transfer of a membrane glycoprotein to the cell surface but does not prevent terminal glycosylation. *Cell* **34**, 233-243.
- McNiven, M. (1998). Dynamin: a molecular motor with pinchase action. *Cell* **94**, 151-154.
- Mizuno, M. and Singer, S. J. (1994). A possible role for stable microtubules in intracellular transport from the endoplasmic reticulum to the Golgi apparatus. *J. Cell Sci.* **107**, 1321-1331.
- Musch, A., Xu, H., Shields, D. and Rodriguez-Boulant, E. (1996). Transport of vesicular stomatitis virus to the cell surface is signal mediated in polarized and nonpolarized cells. *J. Cell Biol.* **133**, 543-558.
- Nakata, T., Terada, S. and Hirokawa, N. (1998). Visualization of the dynamics of synaptic vesicle and plasma membrane proteins in living axons. *J. Cell Biol.* **140**, 659-674.
- Ngoc, S. N., Briquet-Laugier, F., Boulain, C. and Olivo, J. C. (1997). Adaptive detection for tracking moving biological objects in video microscopy sequences. *Proc. IEEE ISIP '97* **3**, 484-487.
- Pagano, R. E., Martin, O. C., Kang, H. C. and Haugland, R. P. (1991). A novel fluorescent ceramide analogue for studying membrane traffic in animal cells: accumulation at the Golgi apparatus results in altered spectral properties of the sphingolipid precursor. *J. Cell Biol.* **113**, 1267-1279.
- Pepperkok, R., Lowe, M., Burke, B. and Kreis, T. E. (1998). Three distinct steps in transport of vesicular stomatitis virus glycoprotein from the ER to the cell surface in vivo with differential sensitivities to GTPγS. *J. Cell Sci.* **111**, 1877-1888.
- Pous, C., Chabin, K., Drechou, A., Barbot, L., Phung-Koskas, T., Settegrana, C., Bourguet-Kondracki, M. L., Maurice, M., Cassio, D.,

- Guyot, M. and Durand, G.** (1998). Functional specialization of stable and dynamic microtubules in protein traffic in WIF-B cells. *J. Cell Biol.* **142**, 153-65.
- Presley, J. F., Cole, N. B., Schroer, T. A., Hirschberg, K., Zaal, K. J. and Lippincott-Schwartz, J.** (1997). ER-to-Golgi transport visualized in living cells. *Nature* **389**, 81-85.
- Rapp, S., Saffrich, R., Anton, M., Jakle, U., Ansorge, W., Gorgas, K. and Just, W. W.** (1996). Microtubule-based peroxisome movement. *J. Cell Sci.* **109**, 837-849.
- Ryan, T. A., Reuter, H. and Smith, S. J.** (1997). Optical detection of a quantal presynaptic membrane turnover. *Nature* **388**, 478-482.
- Scales, S. J., Pepperkok, R. and Kreis, T. E.** (1997). Visualization of ER-to-Golgi transport in living cells reveals a sequential mode of action for COPII and COPI. *Cell* **90**, 1137-1148.
- Sheetz, M. P.** (1996). Microtubule motor complexes moving membranous organelles. *Cell Struct. Funct.* **21**, 369-373.
- Steyer, J. A., Horstmann, H. and Almers, W.** (1997). Transport, docking and exocytosis of single secretory granules in live chromaffin cells. *Nature* **388**, 474-478.
- Traub, L. M. and Kornfeld, S.** (1997). The trans-Golgi network: a late secretory sorting station. *Curr. Opin. Cell Biol.* **9**, 527-533.
- Tsien, R. Y. and Miyawaki, A.** (1998). Seeing the machinery of live cells. *Science* **280**, 1954-1955.
- Wacker, I., Kaether, C., Kromer, A., Migala, A., Almers, W. and Gerdes, H. H.** (1997). Microtubule-dependent transport of secretory vesicles visualized in real time with a GFP-tagged secretory protein. *J. Cell Sci.* **110**, 1453-1463.
- Wiemer, E. A., Wenzel, T., Deerinck, T. J., Ellisman, M. H. and Subramani, S.** (1997). Visualization of the peroxisomal compartment in living mammalian cells: dynamic behavior and association with microtubules. *J. Cell Biol.* **136**, 71-80.
- Yoshimori, T., Keller, P., Roth, M. G. and Simons, K.** (1996). Different biosynthetic transport routes to the plasma membrane in BHK and CHO cells. *J. Cell Biol.* **133**, 247-256.